SCIENCE CHINA
Chemistry

• ARTICLES •

doi: 10.1007/s11426-016-0351-5

Aptamer-based self-assembled supramolecular vesicles for pH-responsive targeted drug delivery

Shuxian Wu[1], Juan Li[1], Hong Liang[1], Liping Wang[1], Xian Chen[1], Guixiao Jin[2*], Xiaoping Xu[1*] & Huang-Hao Yang[1*]

[1]*Key Laboratory of Analysis and Detection Technology for Food Safety of the Ministry of Education, Fujian Provincial Key Laboratory of Analysis and Detection Technology for Food Safety, College of Chemistry, Fuzhou University, Fuzhou 350002, China*
[2]*College of Ecological Environment and Urban Construction, Fujian University of Technology, Fuzhou 350108, China*

Received August 23, 2016; accepted September 21, 2016; published online December 7, 2016

Supramolecular vesicles have received great attention in biomedical application due to their inherent features, including simple synthesis and tunable amphiphilicity of the building blocks. Despite tremendous research efforts, developing supramolecular vesicles with targeted recognition and controlled release remains a major challenge. Herein, we constructed a novel aptamer-based self-assembled supramolecular vesicle by host-guest complexation of pyrene, viologen lipid, and cucurbit[8]urils for pH-responsive and targeted drug delivery. The proposed supramolecular vesicles are easy to be assembled and offer simple drug loading. Based on confocal fluorescence microscopy and cytotoxicity experiments, the drug-loaded supramolecular vesicles were shown to possess highly efficient internalization and apparent cytotoxic effect on target cancer cells, but not control cells. Furthermore, through simple aptamer or drug substitution, supramolecular vesicles can be applied to a variety of target cell lines and drugs, making it widely applicable. Taking advantage of the easy preparation, good stability, rapid pH response, and cell targeting ability, the aptamer-based self-assembled supramolecular vesicles hold great promise in controlled-release biomedical applications and targeted cancer therapy.

aptamer, supramolecular vesicle, pH-responsive, drug delivery

Citation: Wu S, Li J, Liang H, Wang L, Chen X, Jin G, Xu X, Yang HH. Aptamer-based self-assembled supramolecular vesicles for pH-responsive targeted drug delivery. *Sci China Chem*, doi: 10.1007/s11426-016-0351-5

1 Introduction

Vesicles are enclosed structures and predominantly spherical in shape. Due to the flexibility, the hollow vesicles are usually composed of a monolayer or bilayer membrane of natural or synthetic amphiphiles. The membrane can sequester and delivery substances, showing promising applications in drug/gene delivery [1,2] and nanoreactors [3]. Substantial achievements have been made in recent years, especially in stimuli responsive applications [4–6]. For example, Wang and coworkers [4] designed an amphiphilic prodrug capable of self-assembling into vesicles that could decompose and release the drug when triggered by either glutathione or reactive oxygen species. Among the stimuli-responsive vesicles, pH-responsive vesicles have attracted great attention due to their rapidness and simplicity [7,8]. It is worth noting that microenvironment in the tumor tissues is generally more acidic than in normal tissues [9], pH as stimuli in drug delivery system is capable of triggering the release of loaded drugs in cancer cells [10,11].

Conventionally, vesicles are constructed by amphiphiles which contain a hydrophobic tail and a hydrophilic head connected by covalent bonds. The chemical synthesis process

*Corresponding authors (email: jinguixiao2008@126.com; xu@fzu.edu.cn; hhyang@fzu.edu.cn)

is relatively complicated and labor-intensive. Compared to common amphiphiles, supramolecules refer to molecules that are linked by host-guest type interactions [12]. This construction has several advantages, such as simple synthesis and tunable amphiphilicity of the building blocks. Owing to these characteristics, supramolecular vesicles hold great promise in stimuli-responsive drug/gene delivery. The supramolecular vesicles based on pillar[6]arene and guest molecules, have been constructed showing pH, Ca^{2+}, and thermal-responsiveness [13]. However, each pillar[6]arene could only contain one guest molecule, leaving few site to be modified. Instead of using pillar[6]arene, cucurbit[8]urils (CB[8]) have attracted great interest in recent years. CB[8] is a macrocyclic host known to join two guest molecules together with high binding affinity in a non-covalent fashion in aqueous media [14,15], and the supramolecules could be easily modified at two ends as needed. These properties make it ideal as host for assembling into supramolecular vesicles. However, there are only a few reports of supramolecular vesicles based on CB[8] [16].

Cell-specific delivery of anticancer drugs is an important issue in order to improve cancer chemotherapy [17]. Aptamers have received particular attention for their wide recognition ability toward specific molecular targets ranging from small inorganic and organic substances to proteins or cells [18–20]. Compared with other recognition elements, such as antibodies, aptamers have multifarious advantages, such as simple synthesis, good stability and design flexibility, making them promising in targeted drug delivery and targeted treatment [21,22].

Inspired by the advantages of CB[8] and aptamers, we designed a aptamer-based self-assembled supramolecular vesicle for targeted and controlled drug delivery (Figure 1). Aptamer, which specifically binds to epithelial cell adhesion molecule (EpCAM) was used as a model [23]. EpCAM is an ideal antigen for clinical applications in cancer diagnosis, prognosis and therapy, and is overexpressed in most solid cancers, such as breast, colorectal, and gastric cancers [24]. We utilize the pyrene and viologen lipids as guests for CB[8]. Pyrene-labeled aptamers are able to form the supramolecular complex with viologen lipids (synthetic results see Figure 2 and Figure 3) through CB[8] conjugation (Figure 1(a)), since CB[8] can encapsulate the pyrene and viologen lipids at the same time [17]. After conjugation, the supramolecules can self-assemble to form vesicles. Emission spectra indicated a marked quenching of the pyrene fluorescence after addition of the viologen lipid and CB[8] (Figure 1(b), blue line). It is attributed to the electron acceptor-donor interactions between pyrene and viologen moieties inside the CB[8] cavity, proving the formation of a ternary complex inside the CB[8] cavity [17]. In the absence of CB[8], the weak interaction between pyrene and viologen moieties also resulted in a slight reduction of fluorescence intensity (Figure 1(b), green line).

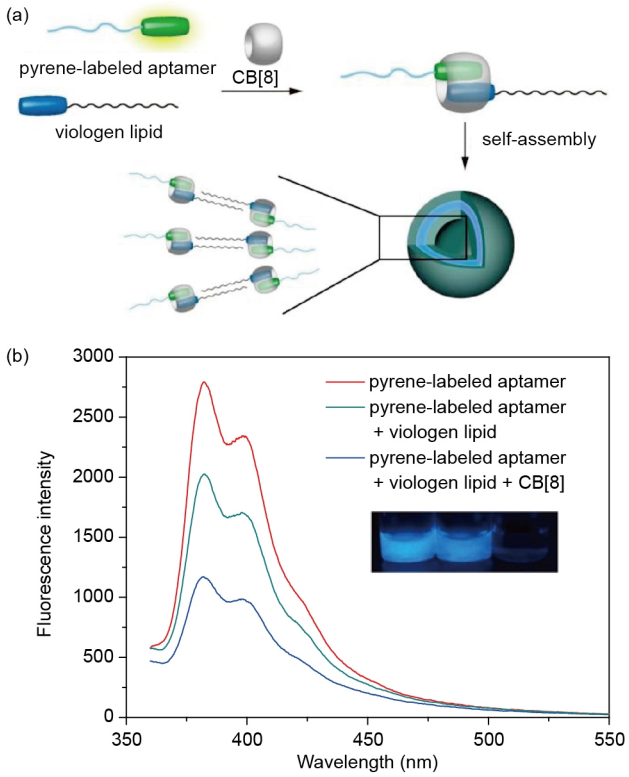

Figure 1 (a) Formation of ternary complex based on pyrene-labeled aptamer, viologen lipid, and CB[8]. (b) Emission spectra of (excited at 303 nm): pyrene-labeled aptamer (25 μM, red line); pyrene-labeled aptamer and viologen lipid (1:1, green line); pyrene-labeled aptamer, viologen lipid and CB[8] (1:1:1, blue line). Inset shows the pictures of vials containing aqueous solution, from left to right: pyrene-labeled aptamer; pyrene-labeled aptamer and viologen lipid (1:1); pyrene-labeled aptamer, viologen lipid and CB[8] (1:1:1) (color online).

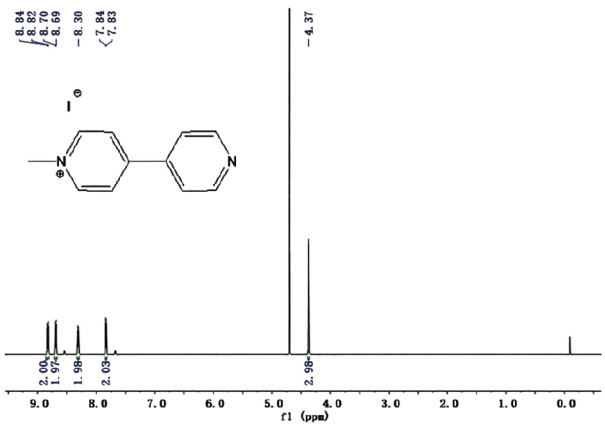

Figure 2 ^{1}H NMR spectra in D_2O at 25 °C of 1-methyl-4,4′-bipyridinium iodide.

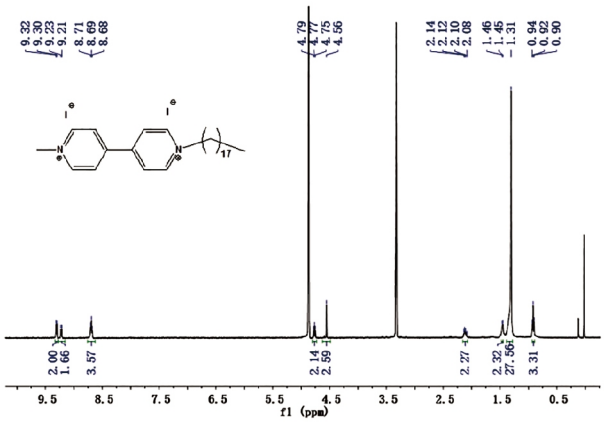

Figure 3 ^{1}H NMR spectra in MeOD at 25 °C of 1-octadecyl-1′-methyl-4,4′-bipyridinium bromide Iodide.

2 Experimental

2.1 Materials and instrument

All reagents including 4,4′-bipyridine, dichloromethane, methyl iodide, ether, methanol, 1-bromooctadecane, acetonitrile, ethanol, CB[8] were purchased from J&K scientific Ltd. (Beijing, China). All chemicals were of analytical grade and used as received without further purification. Cell Counting Kit-8 (CCK-8) was purchased from Dojindo (Japan). The water used in all the preparation was ultrapure, which obtained from a Millipore water purification system (resistivity 18.2 MΩ).

Human normal liver cell line L-02 and breast cancer cell line MCF-7 were obtained by the cell center of our laboratory.

The HPLC-purified pyrene-labeled aptamer and control sequence were synthesized by Takara bio company (Dalian, China) (Table 1). The DNA was dissolved in ultrapure water as stock solutions.

Ultraviolet-visible-near-infrared (UV-Vis-NIR) absorption spectra were collected in a standard 1-cm path length quartz cuvette on an Infinite M200 PRO Microplate Reader (Tecan, Switzerland). Other instruments used in the experiment included fluorospectro photometer F-4600 (Hitachi, Japan), atomic force microscope nanoscope IIId (Veeco, USA), CO_2 incubator Scientific HERAcell 150i (Thermo, USA), confocal microscope C2/C2si (Nikon, Japan), ultrapure water system CascadaTM (Pall, USA), acidimeter Starter 3C (Ohaus, USA), and ultrasonic cleaning instrument (Shumei, China).

Table 1 The DNA sequences employed in this work

Name	Sequence (5′–3′)
EpCAM aptamer	pyrene-AAACACTACAGAGGTTGCGTCTGTC-CCACGTTGTCATGGGGGGTTGGCCTG
Control sequence	pyrene-AAAGGTGTGAAGCTACCGTTGAG-CACCCGGCAAGGAGCUGGAAGGCUGGGA

2.2 Synthesis of 1-methyl-4,4′-bipyridinium iodide

A 500 mL RB flask was charged with 4,4′-bipyridine (10.0 g, 64 mM) in 150 mL dichloromethane. Methyl iodide (5.0 mL, 81 mM) in dichloromethane (50 mL) was added drop-wise to the stirred flask. The mixture was refluxed for 1 h and left to cool with stirring. The yellow product was filtered off, washed with ether, and then purified by recrystallization from methanol for two times, and finally washed with ether again. ^{1}H NMR (400 MHz, D_2O), δ (ppm): 8.83 (d, J=6.8 Hz, 2H), 8.69 (d, J=6.2 Hz, 2H), 8.31 (d, J=6.7 Hz, 2H), 7.83 (d, J=6.3 Hz, 2H), 4.37 (s, 3H).

2.3 Synthesis of 1-octadecyl-1′-methyl-4,4′-bipyridinium bromide iodide

A 50 mL RB flask was charged with 1-methyl-4,4′-bipyridinium iodide (0.6 g, 2 mM), 1-bromooctadecane (3.3 g, 10 mM) and acetonitrile (20 mL). The reaction mixture was heated at reflux for 48 h. A red precipitate was collected and recrystallized using ethanol/water. ^{1}H NMR (400 MHz, MeOD), δ (ppm): 9.31 (d, J=6.0 Hz, 2H), 9.22 (d, J=6.6 Hz, 2H), 8.69 (t, J=6.1 Hz, 4H), 4.77 (m, 2H), 4.56 (s, 3H), 2.11 (q, J=14.5, 8.2 Hz, 2H), 1.46 (d, J=4.4 Hz, 2H), 1.31 (s, 28H), 0.91 (t, J=6.8 Hz, 3H).

2.4 Dox encapsulation

To prepare Atp-vesicles@Dox, 5 mg/mL aqueous solution of doxorubicin (Dox) was quickly added into a freshly prepared aqueous solution of aptamer, CB[8] and viologen lipid, the resulting mixture was sonicated for 30 min, and unloaded Dox molecules were removed by dialysis against water. The Dox encapsulation efficiency was calculated by the following equation.

$$\text{Encapsulation efficiency (\%)} = \left(m_{\text{Dox-loaded}} / m_{\text{Dox}}\right) \times 100\%$$

where $m_{\text{Dox-loaded}}$ and m_{Dox} are mass of Dox encapsulated in vesicles and mass of Dox added, respectively. The mass of Dox was measured by the fluorescence emission spectra which excited at 500 nm, and calculated as relative with a standard calibration curve in the concentrations from 0.01 mg/mL to 1 mg/mL.

2.5 Fluorescence confocal imaging

Human normal liver cell line L-02 and breast cancer cell line MCF-7 were maintained in RPMI 1640 medium supplemented with 15% fetal bovine serum, penicillin (100 unit/mL) and streptomycin (100 μg/mL) at 37 °C in a humidified 5% CO_2 atmosphere. For cell imaging, cells (2×10^5)

were cultured on 35 mm diameter petridish and incubated for 24 h. After cell adhesion, culture media was removed, then culture media which included Atp-vesicles@Dox (the concentration was 300 nM) were added into each dish, and cells were incubated for 1 h. After cell incubation, culture media was removed, and washed with phosphate buffered saline (PBS) three times. Fresh culture media was added in each dish. Finally, the petridishes were detected in fluorescence confocal.

2.6 *In vitro* release of Dox

Apt-vesicles@Dox were incubated in PBS of pH 7.4 and 5.5 over different periods of time 0.5, 1, 2, 4, 6, 8, 12 h. The solution was filtered by 3 kDa filters to wash away released Dox. The fluorescence intensity of Dox was used to calibrate the released Dox concentration.

$$\text{Release rate}\ (\%) = \left(m_{\text{Dox-released}} / m_{\text{Dox-loaded}}\right) \times 100\%$$

where $m_{\text{Dox-released}}$ and $m_{\text{Dox-loaded}}$ are mass of Dox released from vesicles and encapsulated in vesicles, respectively. The mass of Dox was measured by the fluorescence emission spectra which excited at 500 nm, and calculated as relative with a standard calibration curve in the concentrations from 0.01 mg/mL to 1 mg/mL.

2.7 Evaluation of cytotoxicity

For the *in vitro* cell toxicity assay, L-02 cells and MCF-7 cells were plated in 96 well plates for 24 h and added with desired concentrations of Apt-vesicles, Apt-vesicles@Dox, control-vesicles@Dox. After incubation for 1 h, culture media was removed, and washed with PBS three times. Fresh culture media was added in each dish, and cell viability was measured with CCK-8 according to the manufacture's protocol after incubation for 24 h.

$$\text{Cell viability}\ (\%) = (\text{OD}_{\text{treated}} - \text{OD}_{\text{blank}}) / (\text{OD}_{\text{control}} - \text{OD}_{\text{blank}}) \times 100\%$$

where $\text{OD}_{\text{control}}$ was obtained in the absence of vesicles, $\text{OD}_{\text{treated}}$ obtained in the presence of vesicles, and OD_{blank} obtained in the presence of culture medium and CCK-8 solution but without cells. Each result was the average of three wells, and 100% viability was determined from untreated cells.

3 Results and discussion

3.1 Characterization of Apt-vesicles

On account of the amphiphilic nature, after formation of the ternary complex, they can self-assemble to form double-layer vesicles, atomic force microscopy (AFM) images provided direct evidence for the formation of vesicles. As shown in Figure 4(a), the AFM images showed the spherical morphol-

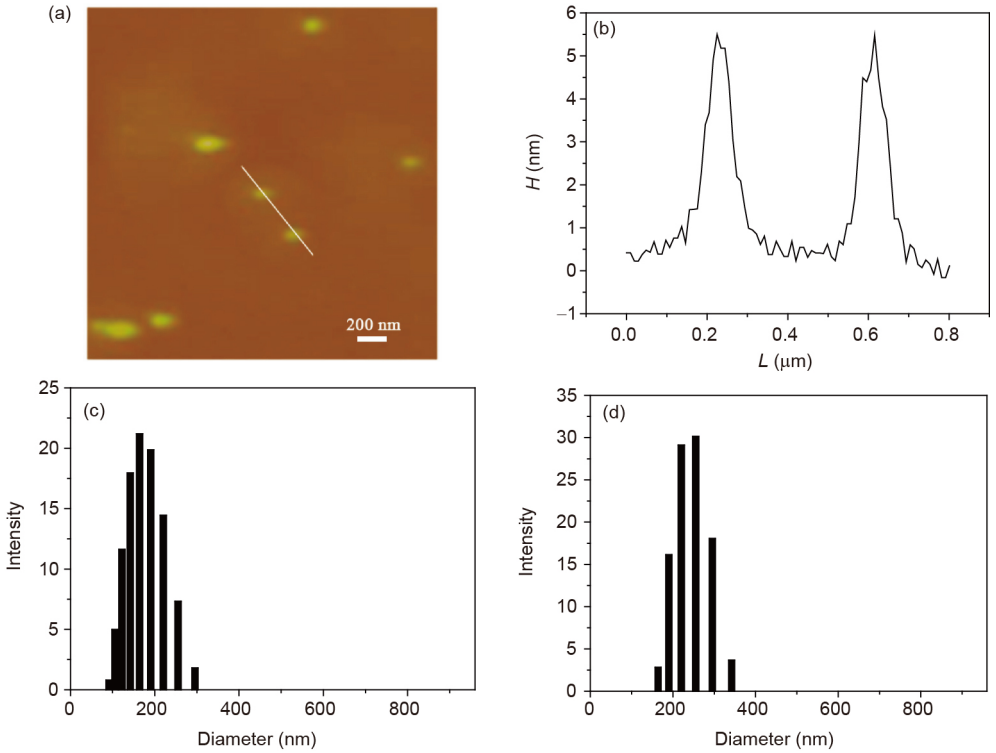

Figure 4 (a) AFM image of the formation of Apt-vesicles (pH 7.4); (b) height of the Apt-vesicles in AFM image; (c, d) DLS data of the Apt-vesicles in different pH solution. (c) pH 7.4; (d) pH 5.0 (color online).

ogy with a diameter ranging from 140 to 220 nm, and the height of the selected vesicles was about 5.5 nm (Figure 4(b)), convincingly indicating the formation of aptamer-based supramolecular vesicles (Apt-vesicles).

For further characterization of Apt-vesicles, we used dynamic light scattering (DLS) to determine the average particle size. DLS revealed that the average hydrodynamic diameter of Apt-vesicles was 180 nm at pH 7.4 (Figure 4(c)). The stability of the Apt-vesicles was investigated and no obvious changes were observed two weeks after preparation (Figure 5). However, when the solution pH was adjusted to 5.0, the average size of Apt-vesicles increased to 280 nm (Figure 4(d)). These results suggested that the Apt-vesicles were responsive to pH.

3.2 Drug release property of the Apt-vesicles

As far as we know, there is no report of the pH-responsive behavior of CB[8]-based supramolecular vesicles. Marquez and coworks [25] used cucurbit[6]uril (CB[6], the homologue of CB[8]) and cyclohexylmethylamine as models to form the supramolecular complex. The pH proved crucial for the kinetics and the rate constants turned out to be related to the degree of protonation of the host and guest. Knowledge of such protonation effects is important in supramolecular chemistry [26,27]. To the Apt-vesicles developed in this experiment, the major driving forces for the Apt-vesicles formation include as follows: (1) charge-transfer interaction between the electron-rich pyrene and the electron-deficient viologen moieties [17,28]; (2) noncovalent interactions such as host-guest interactions [29]. The pH-responsive behavior of Apt-vesicles could be explained when the solution pH changed to acidic, two guest molecules and the polar oxygen atoms in carbonyl groups at the CB[8] portals were easily protonated in acidic condition [25,30], and thereby impact the charge-transfer interaction between two guest molecules, reducing the driving force for formation of supermolecular complex. We presumed this change would induce the incompact packing of drugs in the Apt-vesicles, realizing the pH-responsive release of drugs in tumor acid microenviroment.

To prove this hypothesis, we evaluated the controlled drug release property of the Apt-vesicles. Herein, as a model drug, doxorubicin (Dox), one kind of hydrophobic anticancer drugs and fluorescence dyes, was used to investigate whether Dox could be encapsulated in the vesicles as well as its release behavior upon external stimuli. Compared with unloaded Apt-vesicles solution, the fluorescence of Dox-loaded Apt-vesicles (Apt-vesicles@Dox) solution became much stronger (Figure 6(a)), which represented the characteristic fluorescence of Dox in aqueous solution. Meanwhile, unloaded vesicles present colorless. However, the Apt-vesicles@Dox solution turned to pink after removing unloaded Dox molecules by dialysis, demonstrating that Dox was successfully encapsulated into the vesicles (Figure 6(a)). According to fluorescence emission spectra, the Dox encapsulation efficiency was calculated to be 8.2%, indicating a good drug-loading capability of the above Apt-vesicles. According to the reported supermolecular vesicles [13,17,31], especially the CB[8] supermolecular vesicle designed by Jiao and coworkers [16], we speculate the Apt-vesicles are double-layer vesicles, and the Dox was encapsulated in hollow cavity.

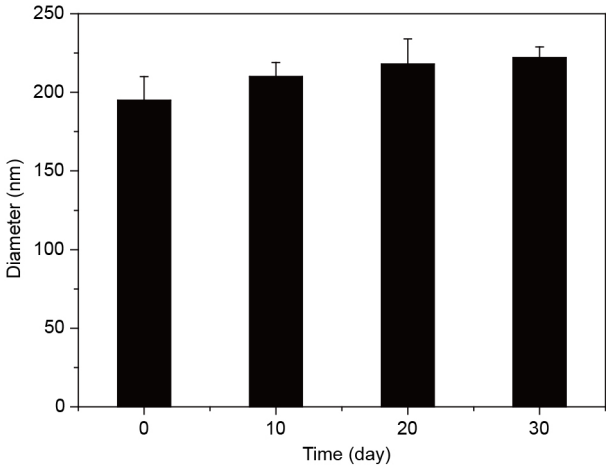

Figure 5 Stability experiment of Apt-vesicles.

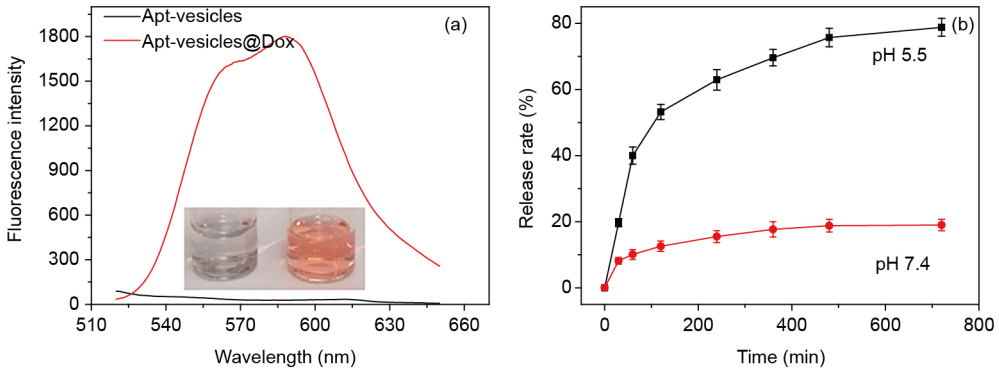

Figure 6 (a) Fluorescence emission spectra of unloaded Apt-vesicles and Apt-vesicles@Dox in water (pH 7.4). Inset shows the pictures of color changes of Apt-vesicles@Dox (right) compared with unloaded Apt-vesicles (left). (b) pH-dependent Dox release from the Apt-vesicles@Dox in different pH solution (excited at 500 nm) (color online).

Subsequently, to characterize the functionality of the pH-sensitive release of Dox, Apt-vesicles@Dox were incubated under different pH, and the release kinetics was investigated. As shown in Figure 6(b), the release of Dox was significantly accelerated by increasing buffer acidity. The cumulative release of Dox was approximately 78.8% at pH 5.5 in the first 12 h. However, the cumulative release of Dox was only 19% within 12 h under the physiological conditions (pH 7.4). It is well documented that most cancer tumor tissues have lower extracellular pH (pH 6.0–7.0) than normal tissues and the bloodstream (pH 7.4), decreasing even more inside cell lysosomes (pH 4.5–5.5) and endosomes (pH 5.5–6.0) [9,32]. Thus, the predictable release of Dox would be facilitated under the increased acidity in both lysosome and endosome, making these pH-responsive vesicles suitable for intracellular drug delivery [31,33].

3.3 Cellular uptake of the Apt-vesicles

To further investigate the cellular uptake of the Apt-vesicles, human normal liver cells L-02 and breast cancer cells MCF-7 were incubated with Apt-vesicles@Dox. MCF-7 cells, which have a high expression of EpCAM, were chosen as target cancer cells, whereas L-02 cells with little EpCAM expressed on the cell membrane were used as control cells. A strong red fluorescence was observed in MCF-7 cells, but very weak fluorescence was seen in L-02 cells (Figure 7(a–d)). The performance of control-vesicles@Dox for L-02 cells and MCF-7 cells were shown in Figure 7(e, f). The results showed that control-vesicles@Dox was hard to enter into L-02 cells and MCF-7 cells without aptamer, which further proved the targeted cellular MCF-7 uptake of Apt-vesicles. Therefore, the introduction of the aptamer recognition element significantly improved the specific targeting of vesicles into target MCF-7 cells.

3.4 Cytotoxicity of Apt-vesicles@Dox

Having shown that Dox could be selectively transported into target cells by Apt-vesicles, the resultant cytotoxicity was evaluated. The cytotoxicity of Apt-vesicles@Dox vs. control-vesicles@Dox in both L-02 and MCF-7 cells was compared, and the results were shown in Figure 8. Unloaded Apt-vesicles exhibited negligible cytotoxicity to both cell lines, indicating good biocompatibility of the proposed Apt-vesicles. Control-vesicles@Dox showed dose-dependent cytotoxicity in both cell lines, since the control DNA could not guide vesicles into cells effectively. In contrast, Apt-vesicles@Dox exhibited efficient and dose-dependent cytotoxicity for MCF-7 cells, but the smaller cytotoxicity for L-02 cells.

Since Apt-vesicles@Dox specifically enters target cancer cells through receptor-mediated endocytosis, thereby providing improved cellular internalization. These findings demonstrate that, under the optimal conditions, Apt-vesicles@Dox are able to selectively kill tumor cells without unwanted toxicity on control cells, which is critical for *in vivo* application of a nanoscale drug-delivery system.

4 Conclusions

In summary, we have successfully constructed novel aptamer-based self-assembled supramolecular vesicles by host-guest complexation of pyrene, viologen lipid, and CB[8] for pH-responsive and targeted drug delivery. The proposed supramolecular vesicles were easy to be assembled and offer simple drug loading. Based on confocal fluorescence microscopy and cytotoxicity experiments, the drug-loaded supramolecular vesicles were shown to possess highly efficient internalization and apparent cytotoxic effect on target cancer cells, but not control cells. Furthermore, through sim-

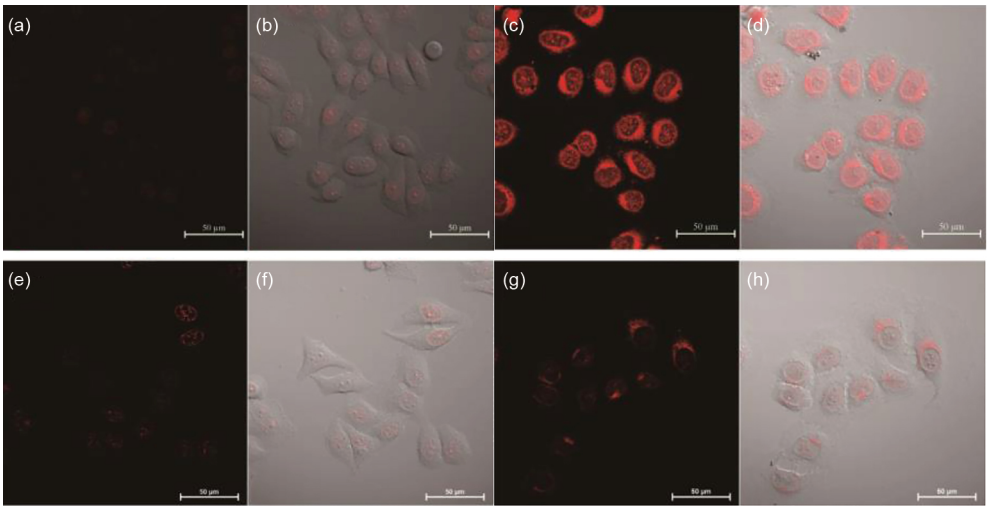

Figure 7 Confocal fluorescence images of (a, b) L-02 cells and (c, d) MCF-7 cells treated with Apt-vesicles@Dox; (e, f) L-02 cells and (g, h) MCF-7 cells treated with control-vesicles@Dox (excited at 543 nm). Scale bar: 50 μm (color online).

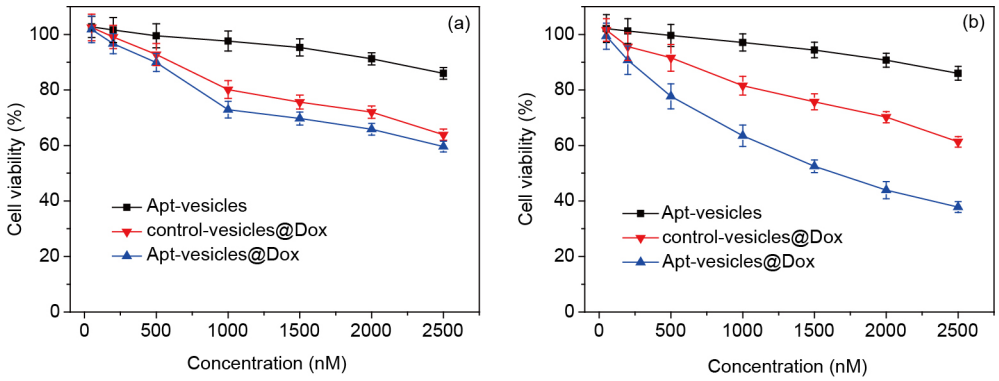

Figure 8 Cytotoxicity of unloaded Apt-vesicles, control-vesicles@Dox and Apt-vesicles@Dox in (a) L-02 cells (control cells) and (b) MCF-7 cells (target cells) (color online).

ple aptamer or drug substitution, supramolecular vesicles can be applied to a variety of target cell lines and drugs, making it widely applicable. Collectively, these simple and versatile supramolecular vesicles have great potential in controlled-release biomedical applications and targeted cancer therapy.

Acknowledgments This work was supported by the National Natural Science Foundation of China (21475026, U1505221, 21505021, 21622502, 21635002), the Natural Science Foundation of Fujian Province of China (2015H6011, 2016J05035), the Program for Changjiang Scholars and Innovative Research Team in University (IRT15R11), and the Independent Research Project of State Key Laboratory of Photocatalysis on Energy and Environment (2014B02).

Conflict of interest The authors declare that they have no conflict of interest.

1 Allen TM, Cullis PR. *Science*, 2004, 303: 1818–1822
2 Guo X, Szoka FC. *Acc Chem Res*, 2003, 36: 335–341
3 Christensen SM, Stamou DG. *Sensors*, 2010, 10: 11352–11368
4 Wang J, Sun X, Mao W, Sun W, Tang J, Sui M, Shen Y, Gu Z. *Adv Mater*, 2013, 25: 3670–3676
5 Song J, Zhou J, Duan H. *J Am Chem Soc*, 2012, 134: 13458–13469
6 Ren T, Liu Q, Lu H, Liu H, Zhang X, Du J. *J Mater Chem*, 2012, 22: 12329–12338
7 Du J, Armes SP. *J Am Chem Soc*, 2005, 127: 12800–12801
8 Rodríguez-Hernández J, Lecommandoux S. *J Am Chem Soc*, 2005, 127: 2026–2027
9 Tannock IF, Rotin D. *Cancer Res*, 1989, 49: 4373–4384
10 Li J, Wu S, Wu C, Qiu L, Zhu G, Cui C, Liu Y, Hou W, Wang Y, Zhang L, Teng IT, Yang HH, Tan W. *Nanoscale*, 2016, 8: 8600–8606
11 Lin LS, Cong ZX, Li J, Ke KM, Guo SS, Yang HH, Chen GN. *J Mater Chem B*, 2014, 2: 1031–1037
12 Yang H, Yuan B, Zhang X, Scherman OA. *Acc Chem Res*, 2014, 47: 2106–2115
13 Cao Y, Hu XY, Li Y, Zou X, Xiong S, Lin C, Shen YZ, Wang L. *J Am Chem Soc*, 2014, 136: 10762–10769
14 Rauwald U, Scherman OA. *Angew Chem Int Ed*, 2008, 47: 3950–3953
15 Kim J, Jung IS, Kim SY, Lee E, Kang JK, Sakamoto S, Yamaguchi K, Kim K. *J Am Chem Soc*, 2000, 122: 540–541
16 Jiao D, Geng J, Loh XJ, Das D, Lee TC, Scherman OA. *Angew Chem Int Ed*, 2012, 51: 9633–9637
17 Li J, Zheng C, Cansiz S, Wu C, Xu J, Cui C, Liu Y, Hou W, Wang Y, Zhang L, Teng I, Yang HH, Tan W. *J Am Chem Soc*, 2015, 137: 1412–1415
18 Yan L, Shi H, He D, He X, Wang K, Xu F. *Sci China Chem*, 2016, 59: 802–808
19 Huang R, Xi Z, He N. *Sci China Chem*, 2015, 58: 1122–1130
20 Li J, Mo L, Lu CH, Fu T, Yang HH, Tan W. *Chem Soc Rev*, 2016, 45: 1410–1431
21 Li L, Hou J, Liu X, Guo Y, Wu Y, Zhang L, Yang Z. *Biomaterials*, 2014, 35: 3840–3850
22 Zhao X, Huang Y, Yang CJ, Mao B. *Sci China Chem*, 2015, 58: 1858–1865
23 Song Y, Zhu Z, An Y, Zhang W, Zhang H, Liu D, Yu C, Duan W, Yang CJ. *Anal Chem*, 2013, 85: 4141–4149
24 Munz M, Baeuerle PA, Gires O. *Cancer Res*, 2009, 69: 5627–5629
25 Marquez C, Nau WM. *Angew Chem Int Ed*, 2001, 40: 3155–3160
26 Ghosh M, Zhang R, Lawler RG, Seto CT. *J Org Chem*, 2000, 65: 735–741
27 Wash PL, Renslo AR, Rebek, Jr. J. *Angew Chem Int Ed*, 2001, 40: 1221–1222
28 Kim HJ, Heo J, Jeon WS, Lee E, Kim J, Sakamoto S, Yamaguchi K, Kim K. *Angew Chem Int Ed*, 2001, 40: 1526–1529
29 Percec V, Glodde M, Bera TK, Miura Y, Shiyanovskaya I, Singer KD, Balagurusamy VSK, Heiney PA, Schnell I, Rapp A, Spiess HW, Hudson SD, Duan H. *Nature*, 2002, 417: 384–387
30 Buschmann HJ, Cleve E, Schollmeyer E. *Inorg Chim Acta*, 1992, 193: 93–97
31 Duan Q, Cao Y, Li Y, Hu X, Xiao T, Lin C, Pan Y, Wang L. *J Am Chem Soc*, 2013, 135: 10542–10549
32 Gerweck LE, Seetharaman K. *Cancer Res*, 1996, 56: 1194–1198
33 Yang X, Grailer JJ, Rowland IJ, Javadi A, Hurley SA, Matson VZ, Steeber DA, Gong S. *ACS Nano*, 2010, 4: 6805–6817